PROPERTIES OF THE CYLINDRICAL RF CAVITY EVALUATION CODE SUPERFISH*

By

K. Halbach, University of California, Lawrence Berkeley Laboratory,
Berkeley, CA 94720; R. F. Holsinger, W. E. Jule, and D. A. Swenson,
University of California, Los Alamos Scientific Laboratory,
P. O. Box 1663, Los Alamos, NM 87545

Summary

A new rf cavity code has been developed that allows evaluation of resonant frequencies and field distributions of the fundamental and higher order modes for practically all conceivable cylindrical geometries. A short description of the procedure to determine these quantities is followed by a discussion of the accuracy of the code, its capabilities, and some applications.

Introduction

The computer code SUPERFISH calculates axisymmetric rf fields (and various secondary quantities), and the associated resonance frequencies, in axisymmetric cavities of otherwise arbitrary shape. It finds these quantities not only for the fundamental, but also for higher modes, and can handle geometries with extreme aspect ratios. Since a detailed derivation and description of the algorithms that make up the heart of the code is being published elsewhere[1] we give here only a summary of the major features of the code pertaining to the determination of the resonance frequency and the associated field distribution. That summary will be followed by some remarks about the use of the code, and the remainder of the paper is devoted to a description of work related to accuracy, comparisons with other codes and actually existing physical structures, established capabilities of the code, and applications.

Field and Resonance Frequency Determination

The problem interior is covered by an irregular triangular mesh, with the boundaries defined by short, straight, mesh lines. The rf fields are described by the azimuthal magnetic field strength H, and Maxwell's equations are represented by one difference equation for H at every mesh point on and inside the boundary. This homogeneous set of linear equations for the values of H at the meshpoints is transformed into a well-posed field evaluation problem by setting H=1 at one (in principle arbitrarily chosen) point, and eliminating the difference equation for that point from the system of equations. The resulting set of inhomogeneous linear equations is solved with a non-iterative Gaussian block elimination and back substitution process. At the point that has been removed from the set of difference equations, the field value H calculated from the now known values of H at the neighboring points will in general be different from the value 1 that was arbitrarily imposed there. This difference, when multiplied by an appropriate factor, can be interpreted as the current I of circulating magnetic charges necessary at that point to drive the cavity (at the chosen frequency) to the field value 1 at that point. Since the coefficients of the original set of difference equations depend on the frequency, this current depends on k = angular frequency/c as well, and a resonance is characterized by I = 0. To find a resonance, we use not I directly, but the normalized quantity $D = 2\pi r_1 kI/\int H^2 dv$. ($r_1$ = distance of the removed point from the axis.) This simplifies the root-finding procedure, since it can be shown that at every resonance, D = 0; $dD/dk^2 = -1$; and that between every two resonances, D = 0 once, with $dD/dk^2 = +1$.

To find a resonance frequency, it takes typically 3-6 evaluations of D. One solution of the difference equations is necessary for each D-evaluation. On the CDC7600 under the Livermore Time Sharing System, it takes $T \approx .75\ 10^{-6}N^2\varepsilon$ (sec) for one such solution. (N represents the total number of meshpoints, and ε the short [mesh] dimension of the problem divided by the long [mesh] dimension.) This time is so short because the coefficient matrix of the system of equations can be partitioned into a block tridiagonal form.

Accuracy

The code has been tested for many numerical effects such as mesh size and geometric configuration. It has been determined how these factors influence the calculation of the resonant frequencies and secondary quantities such as transit time factors, stored energy, etc. These effects have been studied in the fundamental mode as well as in higher modes.

We have used an empty cylindrical cavity for some of our studies since there are analytic solutions for comparison. For the TM_{021} mode (Fig. 1) we find that doubling the mesh size from L/50 to L/25 (where L is the characteristic dimension of the mode) results in a change in the resonant frequency of several parts in 10^4. Also for the TM_{021} mode we have inserted a metallic boundary as shown in Figs. 1.B and 1.C. The frequency is calculated for both the Neumann and Dirichlet boundary conditions at the symmetry plane and it changes by one part in 10^4. The code calculates the empty can frequency also to one part in 10^4. All of these cases have a mesh size of approximately L/50. These figures also illustrate some of the power of this computation, i.e., the information about the field shape of these modes would be very difficult to obtain by measurement.

In Fig. 2 we see the effect of mesh size on frequency for several different geometries and for the TM_{021} mode in the empty can. One sees that the frequency is approaching an asymptotic value for a mesh size of L/60.

Fig. 3 shows a 3 cell and 6 cell cavity, each made up from the 1 cell cavity shown. One sees that the frequencies for the three cases agree

*Work supported by U. S. Energy Research and Development Administration.

to several parts in 10^4. This calculation was done with a relatively coarse mesh as is shown in Fig. 3.D.

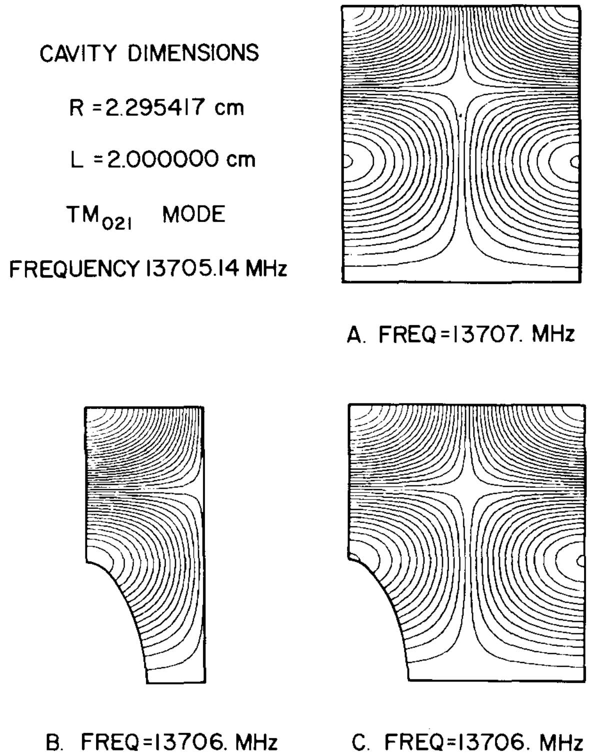

Fig. 1.A Empty can TM_{021} mode.
1.B Modified empty can TM_{021} mode with an electric boundary condition.
1.C Modified empty can TM_{021} mode with a magnetic boundary condition.

Comparisons

We have compared the results calculated by this code to results obtained from measurements on real cavities and to those obtained by other rf cavity codes. The computational results are shown in Table II and the corresponding geometries are given in Table I.

We have two cases of comparison with measured values. These are shown in Figs. 4 and 5. In Figs. 4.A, 4.B, 4.C are shown the field patterns of three modes measured by J. Potter. Also shown there are the measured and calculated values of the frequency for each mode. The agreement is quite good.

Fig. 5 shows two modes in a CTR cavity at LASL. Again the agreement between measurement and calculation is quite good.

Capabilities

This code can solve many problems which could not be easily handled by previously existing codes and in some cases could not be handled at all. The first of these, as has been mentioned, is the ability to solve completely arbitrary boundary shapes as long as they have cylindrical symmetry (Fig. 6). While the input data preparation for

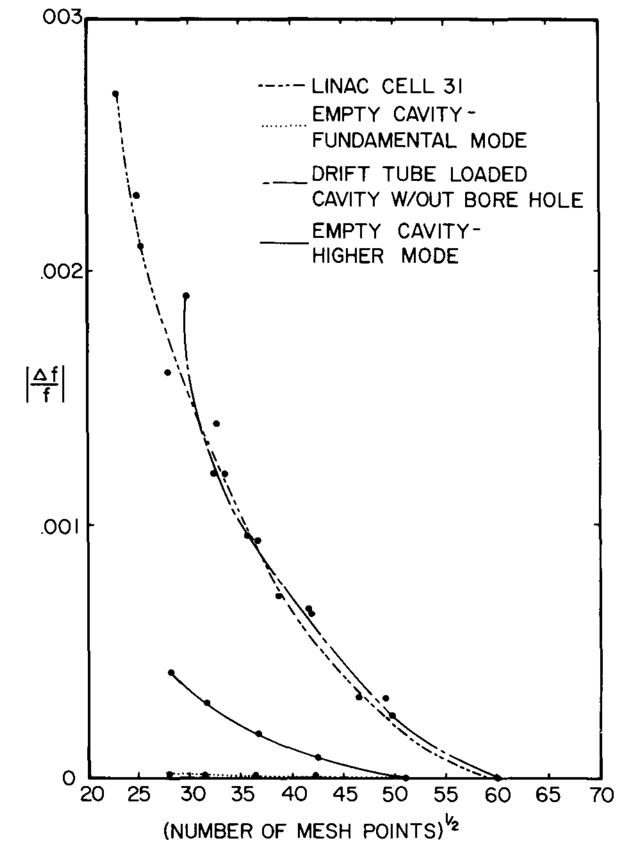

Fig. 2 Mesh dependence for various geometries.

such a geometry would be tedious for the user, the code would not develop indigestion. Secondly, there may be more than one closed region in the problem as in Fig. 3.

Also there is no difficulty in solving severe geometries, i.e., those which have a radial to longitudinal ratio of 30:1. Geometries in this category are low β drift tube linac cavities and multi-cell cavities.

Another feature shown in Fig. 3.D is the ability to have a variable mesh density. This feature allows the solution of larger problems than would be possible with a fixed mesh density. Fig. 3.C is a good example of this.

Another aspect of the code is illustrated in storage ring design. Here, it is desirable to know the frequencies, stored energies, and transit time factors for higher modes than the fundamental. The code can find these modes with ease. Of course the higher the mode, the less accurate is the calculation. In fact, for the modes TM_{071} and TM_{044}, which are the 29th and the 30th modes of the empty can, the analytic values for the frequencies are 1179.9 MHz and 1186.3 MHz while the code finds 1183.0 MHz and 1196.6 MHz. These calculations are done with a mesh spacing which has only 7 mesh points between nodes. Even though these modes are very close together, the code had no trouble in finding them.

TABLE I

SAMPLE LAMPF DRIFT TUBE LINAC GEOMETRIES

PROTON ENERGY	.75	5	10	20	40	60	80	100
Cell Length	6.063	15.694	21.802	30.708	42.620	51.252	58.245	63.643
Cell Diameter	94	94	90	90	90	88	88	88
Gap Length	1.288	4.270	4.229	7.632	13.663	17.977	22.507	26.283
D.T. Diameter	18	18	16	16	16	16	16	16
Corner Radius	2	2	4	4	4	4	4	4
Nose Radius	0.5	0.5	1	1	1	1	1	1
Bore Radius	0.75	0.75	1	1.5	1.5	1.5	1.5	1.5
Face Angle	0	0	0	0	0	0	0	0

SAMPLE LAMPF SIDE COUPLED LINAC GEOMETRIES

PROTON ENERGY	101	202	306	402	501	601	703	800
Cavity Length	8.028	10.586	12.230	13.294	14.120	14.764	15.278	15.660
Cavity Diameter	25.654	25.654	25.527	25.654	25.654	25.908	25.908	25.908
Gap Length	2.544	3.756	4.726	5.322	5.729	6.213	6.468	6.659
Cone Angle	30	30	30	30	30	30	30	30
Outer Radius	3.537	4.817	5.639	6.171	6.584	6.906	7.163	7.354
Blend Radius	1	1	1	1	1	1	1	1
Nose Radius	0.4	0.4	0.4	0.4	0.4	0.4	0.4	0.4
Bore Radius	1.588	1.588	1.905	1.905	1.905	1.905	1.905	1.905
Septum Thickness	0.952	0.952	0.952	0.952	0.952	0.952	0.952	0.952

TABLE II

COMPARISON OF RESULTS (MESSYMESH TO SUPERFISH)

Geometry	DTL .75 MeV		DTL 5 MeV		DTL 10 MeV		DTL 20 MeV	
	MMESH	SFISH	MMESH	SFISH	MMESH	SFISH	MMESH	SFISH
Frequency	200.879	200.395	201.101	200.982	200.69	200.663	200.781	200.839
Power	930	948	2137	2124	3020	3006	4326	4311
Stored Energy	0.0607	0.0619	0.1577	0.1577	0.2074	0.2075	0.2938	0.2941
Shunt Impedance	65.11	63.95	73.34	73.87	72.09	72.51	70.89	71.22
Q Factor	82230	82163	93110	93711	86462	87000	85552	86073
Transit Time								
T	0.721	0.749	0.838	0.842	0.884	0.901	0.854	0.864
TP	0.074	0.069	0.048	0.046	0.035	0.030	0.044	0.041
TPP	0.004	0.004	0.006	0.005	0.004	0.004	0.005	0.005
S	0.518	0.498	0.447	0.436	0.376	0.354	0.427	0.414
SP	0.048	0.050	0.057	0.057	0.051	0.050	0.056	0.055
SPP	0.013	0.012	0.006	0.006	0.004	0.003	0.005	0.005
EZ (Gap Center)	3.027	3.274	3.444	3.557	4.347	4.699	3.649	3.783

Geometry	DTL 40 MeV		DTL 60 MeV		DTL 80 MeV		DTL 100 MeV	
	MMESH	SFISH	MMESH	SFISH	MMESH	SFISH	MMESH	SFISH
Frequency	200.806	200.974	200.545	200.695	200.457	200.52	200.366	200.567
Power	6243	6202	8138	8137	9523	9551	10697	10607
Stored Energy	0.4116	0.4105	0.500	0.5021	0.5743	0.5776	0.6327	0.6327
Shunt Impedance	68.18	68.72	62.89	62.98	61.08	60.98	59.42	60.0
Q Factor	83074	83580	77310	77799	75841	76191	74355	75161
Transit Time								
T	0.800	0.808	0.767	0.775	0.719	0.727	0.677	0.684
TP	0.059	0.057	0.068	0.066	0.081	0.080	0.092	0.091
TPP	0.007	0.007	0.007	0.007	0.008	0.008	0.008	0.008
S	0.503	0.495	0.544	0.537	0.592	0.586	0.628	0.623
SP	0.062	0.062	0.064	0.064	0.065	0.066	0.065	0.065
SPP	0.008	0.008	0.010	0.009	0.013	0.012	0.015	0.015
EZ (Gap Center)	2.7543	2.807	2.3859	2.427	2.050	2.077	1.825	1.851

COMPARISON OF RESULTS (LALA TO SUPERFISH)

Geometry	SCL 101 MeV		SCL 202 MeV		SCL 306 MeV		SCL 402 MeV	
	LALA	SFISH	LALA	SFISH	LALA	SFISH	LALA	SFISH
Frequency	805.000	806.611	805.000	805.056	805.000	805.326	805.000	805.437
Power	1603	1593	1785	1799	2097	2083	2223	2208
Stored Energy	0.0065	0.0064	0.0083	0.0084	0.0103	0.0102	0.0113	0.0112
Shunt Impedance	49.77	50.35	59.25	58.82	58.34	58.70	59.90	60.19
ZT^2	38.33	37.33	47.25	45.97	44.82	44.43	46.113	45.82
Q Factor	20369	20292	23698	23652	24853	24788	25670	25583
Transit Time	0.8776	0.861	0.893	0.884	0.8765	0.870	0.8774	0.873
ZT^2/Q	1882	1840	1994	2256	1803	1792	1796	1791

Geometry	SCL 501 MeV		SCL 601 MeV		SCL 703 MeV		SCL 800 MeV	
	LALA	SFISH	LALA	SFISH	LALA	SFISH	LALA	SFISH
Frequency	805.000	805.395	805.000	805.223	805.000	805.499	805.000	805.953
Power	2352	2336	2409	2383	2499	2466	2571	2534
Stored Energy	0.0121	0.0120	0.0126	0.0125	0.0132	0.0130	0.0136	0.0134
Shunt Impedance	60.11	60.43	61.89	61.97	61.82	61.94	61.67	61.81
ZT^2	46.37	46.33	47.117	47.23	46.933	47.34	46.681	47.33
Q Factor	26046	25961	26665	26573	26802	26732	26873	26846
Transit Time	0.8783	0.876	0.8725	0.873	0.8713	0.874	0.870	0.876
ZT^2/Q	1780	1784	1766	1777	1751	1770	1737	1763

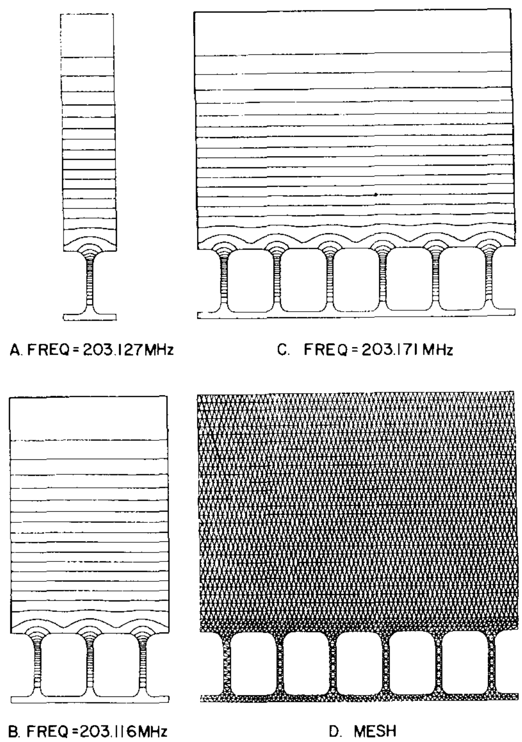

Fig. 3. Cavities to test the sensitivity of large multiple cell configurations.

SIDE COUPLED LINAC STRUCTURE

HIGHER ORDER MODES

FREQUENCIES	MEASURED (MHz)	CALCULATED (MHz)
TM_{010}	804.8	804.5
TM_{011}	1628.6	1626.6
TM_{020}	1885.0	1885.0

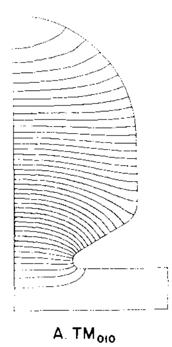

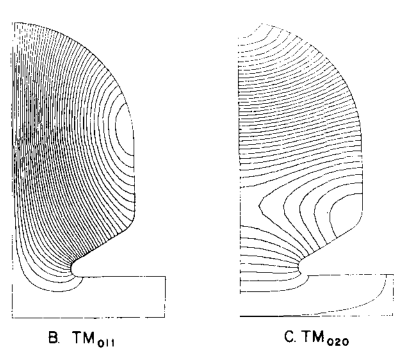

Fig. 4. Measured side coupled linac modes.

A great deal of work has been put into the development of an intelligent root finder for these higher modes, and further work is in progress (for instance, on a "next mode predictor") by one of the authors (KH). In addition, we plan to implement in the near future a procedure that eliminates problems that can arise from an unfortunate choice of the point that has been removed from the initial set of difference equations.

Further work is in progress which will make it possible to specify a desired frequency and iterate on the geometry to produce a cavity which has that frequency.

Applications

Some of the applications that the code is being used for are presented here. First, as already mentioned, it is being used to study higher modes in cavities for the storage ring at BNL. This geometry and several higher modes are shown in Fig. 7.

Another very important structure in which it is necessary to study a higher mode is shown in Fig. 8. This cavity is going to be used in the U.S.S.R. meson facility[3] and is being evaluated for use in the high energy region of a pion generator for medical applications. For this purpose the accelerating mode (Fig.8.A) and the coupling mode (Fig. 8.B) must be brought into confluence. Neither of these modes is the fundamental.

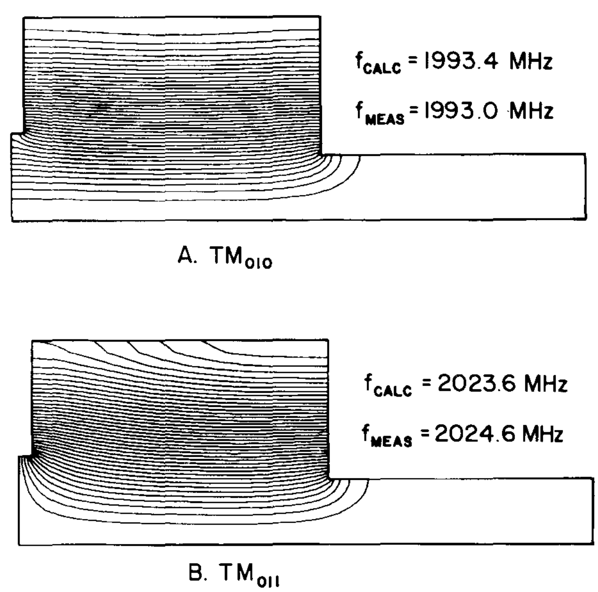

Fig. 5. Measured CTR modes.

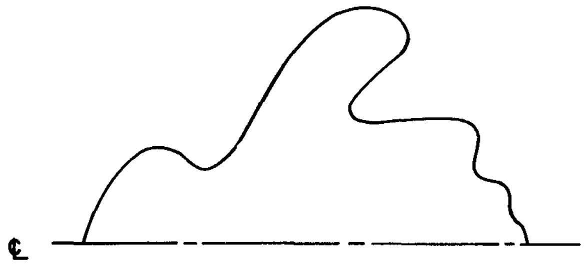

Fig. 6. Example of an arbitrary geometry.

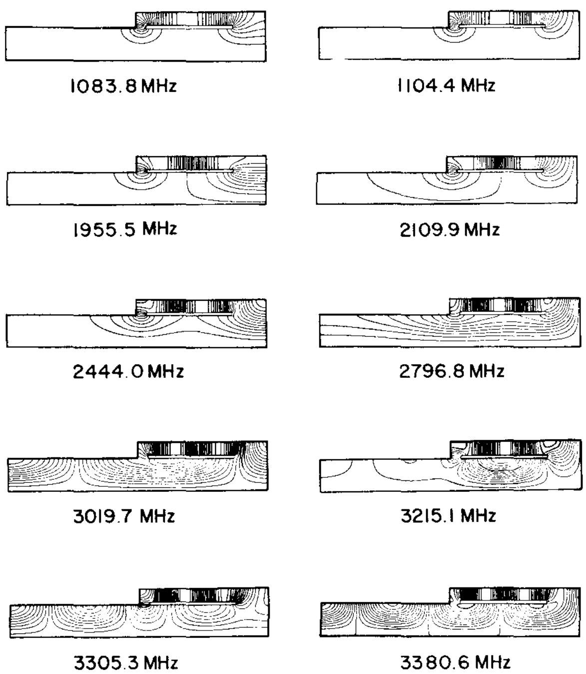

Fig. 7. BNL storage ring cavity - first 10 modes.

Fig. 9.A shows an output cavity and the collector of a 201 MHz klystron. Since the spent beam that enters the collector still contains rf current at the klystron's fundamental frequency and its first few harmonics, it is necessary to determine if the collector resonates at any of these frequencies. A high impedance at a harmonic frequency could cause collector oscillations by reflecting electrons back towards the klystron output cavities. Fig. 9.C shows the fundamental mode of the collector to be greater than four times the frequency of the fundamental mode of the output cavity shown in Fig. 9.B.

We will also use the code to study the field distribution in a multi-cell structure to be used for an alternating phase focused linac.

As a last example, which will demonstrate the extreme power of this code, we present the results of a calculation for the first 15 cells of the first tank of the drift tube linac at LAMPF (Fig. 10). This figure shows the field lines (Fig. 10.A) and the axial electric field (Fig. 10.B) for a non-periodic structure.

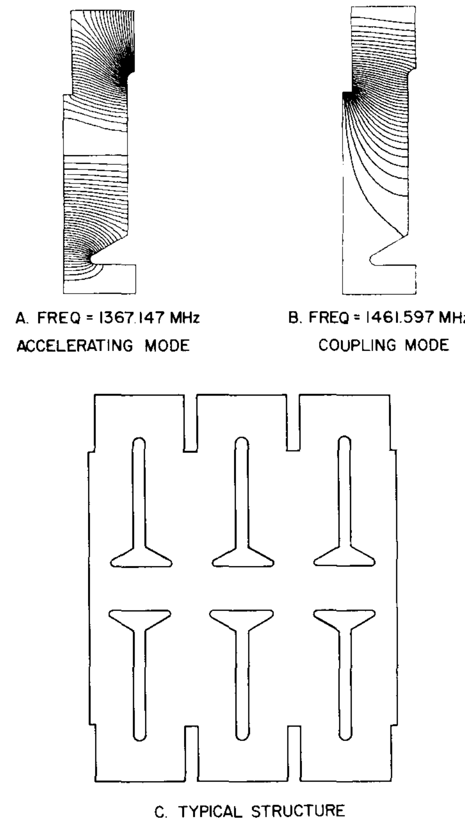

Fig. 8. U.S.S.R. meson factory cavity.

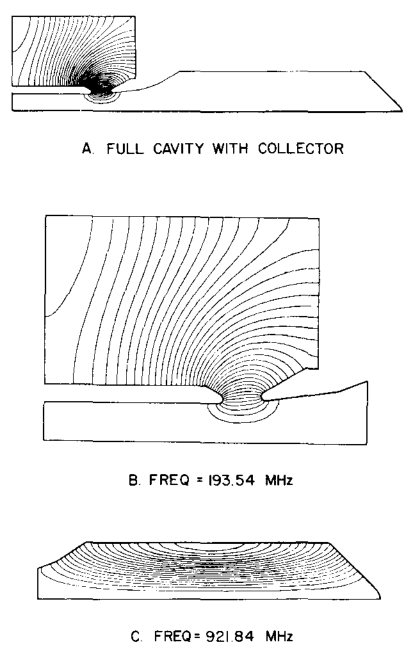

Fig. 9. Klystron cavity.

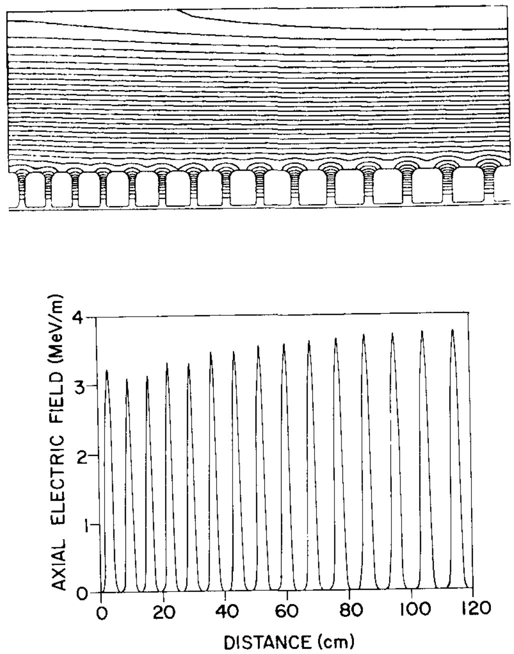

Fig. 10. First 15 cells of tank 1 of the 201 MHz linac.

Acknowledgments

We would like to thank Perry Wechsler for the fine job he did providing computer support and the help he gave us in executing the many tests to which we have subjected the program. We would also like to thank Bob Jameson and Ed Knapp for the continued support they gave which made possible the realization of the project.

References

1. K. Halbach and R.F. Holsinger, "SUPERFISH - a Computer Program for Evaluation of RF Cavities with Cylindrical Symmetry," Particle Accelerators, Gordon and Breach Science Publishers, Ltd., 42 William IV Street, London, WC2, England. (To be published)

2. J.M. Potter, "Transverse Modes in a Resonantly Coupled Accelerator," Proceedings of the 1966 Linear Accelerator Conference, p. 109-114.

3. V.G. Andreev, V.M. Pirozhenko, "Parameters of an Accelerating Structure for Proton Linear Accelerator at Higher Energies," Proceedings of Radiotechnical Institute, Academy of Sciences, U.S.S.R., No. 9, 1971 (Russian edition).

DISCUSSION

P. Morton, SLAC: As I understand it your parameter epsilon is always less than 1. So the weirder your cell is the faster it converges.

Halbach: You can get in trouble with that formula if you don't use it carefully. It looks as if the time to find one field solution goes as the number of mesh points squared. However there is also the ratio of the short dimension divided by the long dimension so another way to say it is: It is the short dimension cubed times the long dimension to the first power which means if you compare the time for a 6 cell cavity with that for a 15 cell cavity the time goes up by only 15 over 6 or 2-1/2.

V. Elyan, RTI: From the results of calculations for the disc and washer structure is there any agreement with the calculations done by Andreev.

Jule: Yes, I think they agreed, fairly well.

Elyan: How much time or manpower did it take you to develop your program?

Halbach: This program was developed in many different steps. We first had a two-dimensional magnet code that had the triangular mesh. Then we developed it into a magnet code for cylindrical problems. Then we needed an rf code and we built a special rf code 6 years ago for the super Hilac that was still using the over-relaxation method. Then Ron Holsinger learned from Chris Iselin of CERN how to use the Gaussian elimination method and wrote the equation solver in about three months. The first version of the new code was developed in one week by combining the existing pieces and implementing the new ideas. That was in March 1976. We have worked on the code on a part-time basis since then and will continue to do so for some time to come.

S. Kulinski, Swierk: Do you think it is possible to use this code in combination with an analytical solution as was done by Warner and Martin?

Halbach: I think it is possible, but the point of the code is that that isn't necessary. The predecessor of this particular code was a combination of a numerical method and an analytical calculation for part of the geometry. That is nice for certain simple geometries. I don't think that method works when you have very complicated geometries and it is the advantage of this code that you just input your geometry and it works.

Kulinski: But in the case of the Alvarez structure you can have very good diminishing of time.

Halbach: You don't have that problem with this code because we don't use over-relaxation, so the field equations are solved very rapidly. It takes about a second or so to solve the field for one Alvarez cell with 1500 mesh points.